arXiv:cond-mat/0403228v1 [cond-mat.mtrl-sci] 9 Mar 2004

Theory of nonlinear optical properties of phenyl-substituted polyacetylenes

Alok Shukla
Physics Department, Indian Institute of Technology, Powai, Mumbai 400076 INDIA

In this paper we present a theoretical study of the third-order nonlinear optical properties of poly(diphenyl)polyacetylene (PDPA) pertaining to the third-harmonic-generation (THG) process. We study the aforesaid process in PDPA's using both the independent electron Hückel model, as well as correlated-electron Pariser-Parr-Pople (P-P-P) model. The P-P-P model based calculations were performed using various configuration interaction (CI) methods such as the the multi-reference-singles-doubles CI (MRSDCI), and the quadruples-CI (QCI) methods, and the both longitudinal and the transverse components of third-order susceptibilities were computed. The Hückel model calculations were performed on oligo-PDPA's containing up to fifty repeat units, while correlated calculations were performed for oligomers containing up to ten unit cells. At all levels of theory, the material exhibits highly anisotropic nonlinear optical response, in keeping with its structural anisotropy. We argue that the aforesaid anisotropy can be divided over two natural energy scales: (a) the low-energy response is predominantly longitudinal and is qualitatively similar to that of polyenes, while (b) the high-energy response is mainly transverse, and is qualitatively similar to that of *trans*-stilbene.

PACS numbers: 78.30.Jw,78.20.Bh,42.65-k

I. INTRODUCTION

Conjugated polymers are believed to be one of the most important materials for the future nonlinear opto-electronic devices[1]. The nonlinear optical response of these materials originates mainly from the π electrons which (a) are delocalized along the backbone of the polymer (b) while being completely localized as far as the motion in a direction transverse to the backbone is concerned. It is this one-electron picture of localized-delocalized π electrons which provides an intuitive understanding of the large response of these materials to external fields. However, the role of electron-correlation effects on the linear and nonlinear nonlinear optical response of conjugated polymers has attracted considerable amount of theoretical attention in recent years, and a number of conjugated polymers such as *trans*-polyacetylene, poly-(para)phenylene (PPP), poly-(para)phenylenevinylene (PPV) etc. have been studied using the Coulomb correlated models in recent works.[2,3,4,5,6,7,8,9] From several of these studies the picture that emerges is that the nonlinear optical properties of various conjugated polymers for the most part are determined by a small number of excited states. For conjugated polymers whose structures are invariant under the inversion operation (centro-symmetric) these states are: (a) $1B_u$, the lowest-energy one-photon state, (b) mA_g, a two-photon state higher in energy than $1B_u$ and with a strong dipole coupling to it, and (c) nB_u, a one-photon state higher in energy than mA_g (but still within the conduction-band threshold), and with strong dipole coupling to it.[2,3,6,8,9] The question is whether this so-called "essential-states picture" is peculiar to a few conjugated polymers, or is it universally shared by all of them?

Recently, optical properties of a new class of conjugated polymers called phenyl-disubstituted polyacetylenes (PDPA's)—which are obtained by substituting the side H atoms of *trans*-polyacetylene by phenyl derivatives—have been the subject of several experimental studies.[10,11,12,13,14,15,16,17] The interesting aspect of the linear optical properties of these materials is that they exhibit strong photoluminescence (PL), despite their structural similarities to *trans*-polyacetylene, which is well-known to be nonphotoluminescent.[14] In a series of theoretical studies, we explained the strong PL exhibited by PDPA's in terms of reduced electron-correlation effects caused by the delocalization of exciton in the transverse direction because of the presence of phenyl rings in that direction.[18,19,20] We also showed that delocalization of exciton also leads to reduction in the optical gaps of these materials as compared to *trans*-polyacetylene.[18,19,20] Moreover, we predicted that the delocalization of excitons will also leave its signatures in form of a significant presence of transverse polarization in the photons emitted during the PL in PDPA's, a prediction, which since then, has been verified in oriented thin-film based experiments.[17]

In the present work, we have undertaken a systematic theoretical study of nonlinear optical properties of PDPA's corresponding to the third-harmonic generation (THG) process. There are several motivations behind the present study, the first of which is studying those excited states of PDPA's which will not be visible in the linear optics. In the THG spectrum of centrosymmetric materials such as PDPA's, A_g-type states appear as two-photon resonances, while the B_u-type states appear as three-photon resonances, thus making the simultaneous exploration of both the symmetry manifolds possible. The next motivation is to explore whether one can understand the nonlinear-optical properties of complex polymers such as PDPA's, in simple terms as enunciated in the essential-states mechanism mentioned above. In particular, for *trans*-polyacetylene, THG spectrum is predicted to have two prominent peaks corresponding to

the essential states mA_g and nB_u mentioned above, in addition to the $1B_u$ peak.[2,3] Therefore, questions arise: (a) How does the nonlinear optical response of PDPA's compare to that of *trans*-polyacetylene? (b) What is the nature of the essential states contributing to the nonlinear optical properties of PDPA's? (c) Will transverse polarization also play a role in the nonlinear optical properties as it did in case of their linear optical properties? The last, but not the least of our motivations behind the present study is to investigate whether one can use conventional computational methods such as configuration-interaction (CI) approach also to study large unit cell materials such as PDPA's (fourteen electrons per cell). This is important in light of the fact that with so many novel and increasingly complex materials being discovered by "nano-technologists" on a routine basis, there will be novel challenges for anyone interested in obtaining their theoretical understanding. Therefore, it is important to apply time-tested theoretical approaches such as the configurations-interaction (CI) method to study these materials to explore whether they can withstand the challenges posed by systems of increasing complexity. We address all these issues by performing calculations on oligo-PDPA's of the third-order nonlinear optical susceptibilities corresponding to the THG process using both the independent-particle Hückel model, as well as Coulomb-correlated Pariser-Parr-Pople (P-P-P) model. The P-P-P model-based calculations were performed using the CI methodology, and approaches such as multi-reference-singles-doubles CI (MRSDCI), and quadruples-CI (QCI) were used to compute the THG spectra. For the Hückel model calculations, we considered oligomers of PDPA's containing up to fifty unit cells, while for P-P-P model calculations up to ten unit cell oligomers were considered. We computed susceptibility component where all photons involved were polarized in the chain direction (longitudinal component), as well as the component where the photons were polarized perpendicular to the chain (transverse component). We see that the THG spectrum is clearly divided over two distinct energy scales: (a) the low-energy response is primarily concentrated in the longitudinal component and is qualitatively similar to that of *trans*-polyacetylene, while (b) the high-energy response is concentrated mainly in the transverse component and is similar to that of *trans*-stilbene. Upon examining the orbitals involved in these responses we conclude that it is the low-energy chain-like molecular orbitals (MOs) close to the Fermi level which are active in the longitudinal component, while the transitions among the chain-like and high-energy phenyl-based orbitals give rise to the transverse component of the response.

The remainder of this paper is organized as follows. In section II we briefly describe the theoretical methodology used to perform the calculations in the present work. Next in section III we present and discuss the calculated nonlinear optical susceptibilities of oligo-PDPA's. Finally, in section IV we summarize our conclusions.

II. METHODOLOGY

The unit cell of PDPA oligomers considered in this work is presented in Fig. 1. Ground state geometry of PDPA's, to the best of our knowledge, is still unknown. However, from a chemical point of view, it is intuitively clear that the steric hindrance would cause a rotation of the side phenyl rings so that they would no longer be coplanar with the polyene backbone of the polymer. The extent of this rotation is also unknown, however, it is clear that the angle of rotation has to be less than 90 degrees because that would effectively make the corresponding hopping element zero, implying a virtual disconnection of the side phenyl rings from the backbone. In our previous works[18,19,20], we argued that the steric hindrance effects can be taken into account by assuming that the phenyl rings of the unit cell are rotated with respect to the y-axis by 30 degrees in such a manner that the oligomers still have inversion symmetry. It is obvious that along the direction of conjugation (longitudinal direction), PDPA is structurally similar to *trans*-polyacetylene, with alternating single and double bonds. But, perpendicular to the conjugation direction (transverse direction), the material has features in common with *trans*-stilbene, with its two phenyl rings, and vinylene-like linkage connecting them. In the following, we will adopt the notation PDPA-n to denote a PDPA oligomer containing n unit cells of the type depicted in Fig. 1.

The point group symmetry associated with *trans*-polyacetylene (and polyenes) is C_{2h} so that the one-photon states belong to the irreducible representation (irrep) B_u, while the ground state and the two-photon excited states belong to the irrep A_g. Because of the phenyl group rotation mentioned above, the point group symmetry of PDPA's is C_i so that its ground state and the two-photon excited states belong to the irrep A_g, while the one-photon excited states belong to the irrep A_u. However, to facilitate direct comparison with polyenes, we will refer to the one-/two-photon states of PDPA's also as B_u/A_g-type states.

The independent-electron calculations on the oligomers PDPA-n were performed using the Hückel model Hamiltonian which, adopting a notation identical to our previous works[18,19,20] reads,

$$H = H_C + H_P + H_{CP}, \tag{1a}$$

where H_C and H_P are the one-electron Hamiltonians for the carbon atoms located on the *trans*-polyacetylene backbone (chain), and the phenyl groups, respectively, H_{CP} is the one-electron hopping between the chain and the phenyl units. The individual terms can now be written as,

$$H_C = -\sum_{\langle k,k'\rangle,M} (t_0 - (-1)^M \Delta t) B_{k,k';M,M+1}, \tag{1b}$$

$$H_P = -t_0 \sum_{\langle\mu,\nu\rangle,M} B_{\mu,\nu;M,M}, \tag{1c}$$

and

$$H_{CP} = -t_\perp \sum_{\langle k,\mu\rangle,M} B_{k,\mu;M,M,}. \tag{1d}$$

In the equation above, k, k' are carbon atoms on the polyene backbone, μ,ν are carbon atoms located on the phenyl groups, M is a unit consisting of a phenyl group and a polyene carbon, $\langle ...\rangle$ implies nearest neighbors, and $B_{i,j;M,M'} = \sum_\sigma (c^\dagger_{i,M,\sigma} c_{j,M',\sigma} + h.c.)$. Matrix elements t_0, and $t_\perp$ depict one-electron hops. In H_C, Δt is the bond alternation parameter arising due to electron-phonon coupling. In H_{CP}, the sum over μ is restricted to atoms of the phenyl groups that are directly bonded to backbone carbon atoms. There is a strong possibility that due to the closeness of the phenyl rings in the adjacent unit cells, there will be nonzero hopping between them, giving rise to a term H_{PP} in the Hamiltonian above. However, in our earlier study,[19] we explored the influence of this coupling on the linear optics of these materials, and found it to have insignificant influence. Therefore, in the present study, we believe that we are justified in ignoring the phenyl-phenyl coupling.

As far as the values of the hopping matrix elements are concerned, we took $t_0 = -2.4$ eV, while it is imperative to take a smaller value for $t_\perp$, because of the twist in the corresponding bond owing to the steric hindrance mentioned above. We concluded that for a phenyl group rotation of 30 degrees, the maximum possible value of $t_\perp$ can be -1.4 eV.[18] Bond alternation parameter $\Delta t = 0.45$ eV was chosen so that the backbone corresponds to *trans*-polyacetylene with the optical gap of 1.8 eV in the long chain limit.

The THG process in oligo-PDPA's were studied by computing the third-order nonlinear susceptibilities $\chi^{(3)}(-3\omega;\omega,\omega,\omega)$. For short we will refer to this susceptibility, as $\chi^{(3)}_{THG}$. First the Hückel Hamiltonian for the corresponding oligo-PDPA was diagonalized to compute the one-electron eigenvalues and eigenfunctions. These quantities were subsequently used in the formulas derived by Yu and Su,[25] to compute $\chi^{(3)}_{THG}$.

The correlated calculations on the oligomers PDPA-n were performed using the P-P-P model Hamiltonian

$$H = H_C + H_P + H_{CP} + H_{ee}, \tag{2}$$

where H_C, H_P, H_{CP} have been explained above. H_{ee} depicts the electron-electron repulsion and can be written as

$$H_{ee} = U \sum_i n_{i\uparrow} n_{i\downarrow} + \frac{1}{2} \sum_{i\neq j} V_{i,j} (n_i - 1)(n_j - 1) \tag{3}$$

where i and j represent all the atoms of the oligomer. The Coulomb interactions are parameterized according to the Ohno relationship[21],

$$V_{i,j} = U/\kappa_{i,j} (1 + 0.6117 R^2_{i,j})^{1/2}\ , \tag{4}$$

where, $\kappa_{i,j,M,N}$ depicts the dielectric constant of the system which can simulate the effects of screening, U is the on-site repulsion term, and $R_{i,j}$ is the distance in Å between the ith carbon and the the jth carbon. The Ohno parameterization initially was carried out for small molecules, and, therefore, it is possible that the Coulomb parameters for the polymeric samples could be somewhat smaller due to interchain screening effects.[22] Since the results obtained will clearly depend on the choice of the Coulomb parameters, we tried two sets: (a) "standard parameters" with $U = 11.13$ eV and $\kappa_{i,j} = 1.0$, and (b) "screened parameters" with $U = 8.0$ eV and $\kappa_{i,i,M,M} = 1.0$, and $\kappa_{i,j,M,N} = 2.0$, otherwise. Using the screened parameters, Chandross and Mazumdar[22] obtained better agreement with experiments on excitation energies of PPV oligomers, as compared to the standard parameters. Recently, we performed a large-scale correlated study of singlet and triplet excited states in oligo-PPV's and observed a similar trend.[23]

As far as the hopping matrix elements for PDPA's and polyenes are concerned, they were assigned the values used in the Hückel-model calculations, except for the bond-alternation parameter for which the smaller value $\Delta t = 0.168$ eV, consistent with the P-P-P model, was used. In *trans*-stilbene, for phenyl rings hopping value of -2.4 eV was used, while in the vinylene linkage the values used were -2.2 eV for the single bond, and -2.6 eV for the double bond. In all the calculations, C-C bond length of 1.4 Å was used for the phenyl rings. In polyenes and PDPA's, along the backbone the single bonds and the double bonds were taken to be 1.45 Å and 1.35 Å, respectively. The bond connecting the backbone to the substituent phenyl rings was taken to be 1.40 Å. In *trans*-stilbene, in the vinylene linkage, the single (double) bond lengths were taken to be 1.54 Å (1.33 Å). The bond lengths used in this paper are the same as the ones used in our earlier works.[18,19,20,23]

The starting point of the correlated calculations for various oligomers were the restricted Hartree-Fock (HF) calculations, using the P-P-P Hamiltonian. The many-body effects beyond HF were computed using different levels of the configuration interaction (CI) method, namely, quadruples-CI (QCI), and the multi-reference singles-doubles CI (MRSDCI). Since the number of electrons in oligo-PDPA's is quite large despite the P-P-P approximation owing to the large unit cell, it is not possible to include all the orbitals in the many-body calculations. Therefore, one has to reduce the number of degrees of freedom by removing some orbitals from the many-body calculations. In order to achieve that, for each oligomer we first decided as to which occupied and the virtual orbitals will be active in the many-body calculations based upon: (a) their single-particle HF en-

ergies with respect to the location of the Fermi level, and (b) Mulliken populations of various orbitals with respect to the chain/phenylene-based atoms. Because of the particle-hole symmetry in the problem, the numbers of active occupied and virtual orbitals were taken to be identical to each other, with the occupied and virtual orbitals being particle-hole symmetric. The remaining occupied orbitals were removed from the many-body calculations by the act of "freezing", i.e., by summing up their interactions with the active electrons, and adding this effective potential to the one-electron part of the total Hamiltonian. The inactive virtual orbitals were simply deleted from the list of orbitals. When we present the CI results on various oligo-PDPA's, we will also identify the list of active orbitals. During the CI calculations, full use of the spin and the point group (C_i for PDPA's) symmetries was made. From the CI calculations, we obtain the eigenfunctions and eigenvalues corresponding to the correlated ground and excited states of various oligomers. Using the many-body wave functions, we compute the matrix elements of the dipole operator amongst various states. Finally, these quantities are fed in to the sum-over-states formulas of Orr and Ward,[26] to obtain the correlated values of $\chi^{(3)}_{THG}$. More details about the procedural aspects of various CI approaches used by us can be found in our earlier works.[19,20,23,24]

III. RESULTS AND DISCUSSION

In this section we present our results on $\chi^{(3)}_{THG}$ using various approaches. First we present and briefly discuss the results computed using the Hückel model, followed by the results computed using various CI approaches.

A. Independent-electron theory

1. Longitudinal Component

Here we present and discuss the longitudinal THG spectrum for the case of oligomer PDPA-50, which has 700 sites leading to 350 occupied and the same number of virtual orbitals. Even within the one-electron theory, calculation of $\chi^{(3)}$'s with such a large number of orbitals is intractable. Therefore, to perform such calculations on larger oligomers, it is mandatory that some of the orbitals be discarded. To this end we adopted the criterion to discard those occupied and virtual orbitals which are more than 3.0 eV away from the Fermi energy. The choice of 3.0 eV is based upon the magnitude of the optical gap and the location of various features in the $\chi^{(3)}$ spectra of smaller oligomers. Since, on PDPA-30 it was also possible to perform exact calculations, we were able to compare our approximate results with the exact ones for that oligomer. We found that the approximate results on longer oligomers are quite accurate.

The total magnitude of component of the longitudinal component of THG susceptibility ($|\chi^{(3)}_{xxxx}(-3\omega;\omega,\omega,\omega)|$), as a function of the incident photon energy E, for fifty unit cell oligomers of PDPA and *trans*-polyacetylene is plotted in Fig. 2. From the figure it is clear that the main peak of the spectrum for both these materials is the first one corresponding to the lowest optically allowed state $1B_u$, and is located at $\hbar\omega = E_g/3$, where E_g is the value of the optical gap defined as $E_g = E(1B_u) - E(1A_g)$. From the figure it is obvious that: (a) qualitatively speaking, longitudinal THG spectra for the both the polymers are similar (b) from a quantitative point of view, as expected, the resonant features of the PDPA spectrum are red shifted as compared to the *trans*-polyacetylene ones (c) in the frequency region of interest, both the resonant, and the off-resonant, nonlinear optical responses of PDPA are much more intense as compared to *trans*-polyacetylene. Since the $1B_u$ state of PDPA's in Hückel model originates from the excitation $HOMO \rightarrow LUMO$, both of which are chain-based orbitals, one can safely conclude that as far as the longitudinal nonlinear-optical response computed at the Hückel level is concerned, oligo-PDPA's behave as if they were smaller band-gap polyenes.

2. Transverse Component

The transverse THG spectrum of oligo-PDPA's saturates very rapidly with size because with increasing conjugation length, the *trans*-stilbene-like structure of the oligomer in the transverse direction is unchanged. With increasing conjugation length, only the overall intensity in the transverse direction is expected to increase, with little change in the qualitative feature. Therefore, here we present the exact results on $|\chi^{(3)}_{yyyy}(-3\omega;\omega,\omega,\omega)|$ for the oligomer PDPA-30 in Fig. 3. It is clear from the figure that there is only one resonant feature in the spectrum and it is located close to 1.7 eV and its intensity is about one-fifth that of the largest resonant intensity in the longitudinal THG spectrum(cf. Fig. 2). Even for smaller oligomers such as PDPA-10 and PDPA-20, the location of the resonance is the same pointing to its possible origins in the phenyl-based orbitals. Therefore, to simplify our task of locating these orbitals, we investigate the THG spectrum of PDPA-10 for which the main peak occurs at 1.71 eV, corresponding to an A_g type state, obtained from the ground state by single-excitations $H \rightarrow L+39$ and $H-39 \rightarrow L$. To investigate the nature of the orbital corresponding to the $L+39$-th one-electron state, we calculated the contribution of the charge density centered on the backbone carbon atoms, to its total normalization. The contribution was computed to be 0.05 which indicates that the orbital in question is predominantly centered on the side phenyl rings. Further investigation of the orbital coefficient reveals that the orbitals in question, are derived from the phenyl-based delocalized (d^*) virtual orbitals,

with no contribution from the localized orbitals (l^*-type) of the phenyl rings. Similarly, owing to the particle-hole symmetry, $H-39$-th orbital is derived from the d-type occupied orbitals of the phenyl rings. The investigation of longer oligomers yields identical results. Thus it is clear that the transverse THG susceptibility of the system owes its origins to phenyl-based delocalized (d/d^*) levels. This is an important point which also helps us perform effective correlated calculations of this component, presented in the next section.

B. Correlated-electron theory

Since the smaller energy gaps obtained with the screened parameters in our earlier works were found to be in much better agreement with the experiments, we will present our main results based upon screened-parameter-based calculations. However, when we compare the PDPA nonlinear optical spectra with those of polyenes, we will use the standard parameters because screened parameters are not valid for polyenes.

1. Longitudinal Component

Now we present correlated calculations for the longitudinal component of the third-harmonic generation susceptibility $\chi^{(3)}_{xxxx}(-3\omega;\omega,\omega,\omega)$ for oligo-PDPA's, performed using the QCI method. Given the large number of electrons in these systems, QCI method is not feasible for them if all the orbitals of the system are retained in the calculations. Since the longitudinal nonlinear optical properties are determined by low-lying excited states of the system, in the limited CI calculations we decided to include the orbitals closest to the Fermi level. Therefore, for PDPA-n we included n occupied, and n virtual orbitals closest to the Fermi level in the QCI calculations. Remaining occupied orbitals were frozen and virtual orbitals were deleted as explained in section II. Thus, the computational effort associated with the QCI calculations on PDPA-n is same as that needed for a polyene with n double bonds. Although for PDPA-10, it leads to Hilbert space dimensions in excess of one million, however, using the methodology reported in our earlier works[19,23], we were able to obtain low-lying excited states of such systems.

The longitudinal THG spectra ($|\chi^{(3)}_{xxxx}(-3\omega;\omega,\omega,\omega)|$) for PDPA-5 and PDPA-10 employing the screened parameters and the QCI method are presented in Figs.4(a) and 4(b), respectively. From the figures it is obvious that the spectra for PDPA-5 and PDPA-10 containing four main features each are qualitatively quite similar, suggesting the possibility that an oligomer as small as PDPA-5 may possess essential features of bulk PDPA. It is clear from Fig. 4 that: (a) The intensity of the nonlinear response increases with the increasing length of the oligomer, and (b) the peaks of the oligomers are redshifted with the increasing conjugation length. Next we examine these peaks in detail.

The properties of excited states contributing to the longitudinal THG spectra of PDPA-5 and PDPA-10 are presented in table I. From the table, and Fig. 4, it is clear that there are three B_u-type states, $1B_u$, nB_u, and kB_u along with two A_g-type states, $2A_g$ and mA_g which contribute, respectively, to the three-photon and two-photon resonances in the spectra. Upon comparing the wave functions of various excited states of PDPA-5, with those of PDPA-10, we infer that qualitatively the wave functions are very similar. For each oligomer, $1B_u$ state, which constitutes the first peak of the spectrum consists mainly of across-the-gap, single excitation. The next peak corresponds to the nB_u state which, for both the oligomers, also consists mainly of higher energy single excitations. The third three-photon resonance corresponding to a still higher energy state labeled kB_u, is a mixture of both singly- and doubly-excited configurations. For PDPA-10, this state is dominated by a high-energy single excitation with important contributions from double excitations, while in PDPA-5 the situation is reverse with main contributions coming from the double excitations. Next, when we examine the wave functions of the states $2A_g$ and mA_g contributing to the two-photon features, we find that configurations contributing to them are essentially identical. However, because of the orthogonality constraint, the relative signs of the coefficients of these configurations are opposite for the two states. One strange aspect of the THG spectrum presented in Fig. 4 is the coincidence of the two-photon and three-photon resonances corresponding to states nB_u and $2A_g$, respectively, for both PDPA-5 and PDPA-10. This is because for both the oligomers, $E(nB_u)/3 \approx E(2A_g)/2$. One wonders whether this is an artifact of using a truncated orbital set in the QCI calculations, or a genuine effect. In order to perform correlated calculations of the transverse THG spectrum of PDPA-5, we used an extended orbital set and performed large-scale MRSDCI calculations presented later in Fig. 7. From there it is clear that although both $2A_g$ and nB_u make important contributions to the spectrum, however, their peaks are well separated, and the intensity of nB_u is much higher than that of $2A_g$, leading us to conclude that the coincidence of $2A_g/nB_u$ peaks in the QCI/THG spectrum is an artifact.

Next we compare the longitudinal THG spectrum of PDPA-10 with that of a polyene consisting of ten double bonds (PA-10), computed using the QCI method, and the standard parameters in the P-P-P Hamiltonian. The spectra are presented in Fig. 5, while the properties of the excited states contributing to the spectra are illustrated in table II. It is clear from that the intensity of the PDPA-10 spectrum is generally larger and all its major peaks are significantly redshifted as compared to the *trans*-polyacetylene oligomer, in agreement with the Hückel model results. Moreover, the THG spectrum of PDPA-10 computed with the standard parameters, still has four main peak corresponding to the states $1B_u$,

nB_u, kB_u, and mA_g, in agreement with the screened-parameter results. The main difference in the THG spectrum of PDPA-10 computed with standard parameters, as compared to the one computed with the screened parameters, is that there is no contribution to it from the $2A_g$ state. When we compare this aspect of PDPA-10 standard parameter THG spectrum with that of PA-10, we find that the PA-10 spectrum also does not exhibit any feature corresponding to $2A_g$. Moreover, PA-10 THG spectrum has only three peaks corresponding to $1B_u$, nB_u, and mA_g, with no peak corresponding to a kB_u-type state. If we compare the wave functions of these three states of PA-10 with those of PDPA-10 (table II), we find that the wave functions of $1B_u$ and mA_g states are very similar to each other for the two materials. As far as the nB_u state is concerned, its wave function for PDPA-10 is composed predominantly of single excitations, while for PA-10 it exhibits large configuration mixing, with significant contribution also coming from the double excitations. Moreover, in PDPA-10, the nB_u state is very close energetically to the mA_g state (slightly below it), while in PA-10, it is much higher in energy than the nB_u state. Note that the nB_u state of PDPA-10 computed with the screened parameters is slightly above the mA_g state (table I). Therefore, the location of the nB_u state is an interesting difference between PA-10 and PDPA-10 which these standard-parameter-based calculations suggest, and it merits further investigation in possibly more extensive calculations. Thus, experimental investigations of the longitudinal THG spectrum of PDPA-10 could possibly shed some light on the following aspects: (a) whether or not the $2A_g$ state makes an important contribution to the spectrum indicating as to what range of Coulomb parameters (screened/standard) are valid for the material, (b) location of nB_u vis-a-vis mA_g, and (c) whether or not there is a peak corresponding to the kB_u state in PDPA's.

2. *Transverse Component*

Performing accurate correlated calculations of $\chi^{(3)}_{yyyy}(-3\omega;\omega,\omega,\omega)$ for oligo-PDPA's is an extremely difficult task. The reason being that the many-body A_g-type states which contribute to the peaks in this component of the susceptibility are very high in energy, and hence are more difficult to compute by many-body methods, as compared to the low-lying excited states contributing to the longitudinal spectra. The very high excitation energies of these states are due to the fact that these A_g-type states are predominantly composed of excited configurations involving high-energy delocalized orbitals originating from the phenyl substituents. However, during our independent-electron study, we concluded that transverse susceptibilities exhibit rapid saturation with the conjugation length. Therefore, we restrict our study of the transverse components of the nonlinear susceptibilities to PDPA-5. We perform calculations with the screened parameters and the MRSDCI method employing thirty orbitals in all, of which fifteen were occupied orbitals, and the remaining fifteen were the virtual ones. Rest of the occupied orbitals were frozen. Of the thirty orbitals, ten were the orbitals closest to the Fermi level which were also used in the QCI calculations. Remaining twenty orbitals were the d/d^*-type phenylene-ring-based orbitals closest to the Fermi level. In the MRSDCI calculations, no l/l^*-type phenylene orbitals were used because they do not make any significant contribution to the transverse nonlinear spectra in the Hückel model calculations. In the MRSDCI calculations, we used 25 reference configurations for the A_g-type states, and 24 for the B_u-type states leading to CI matrices of dimensions close to half-a-million both for the A_g and B_u manifolds.

The transverse THG spectrum of PDPA-5, along with the THG spectrum of *trans*-stilbene (labeled PPV-2) oriented along the y-axis computed using the QCI approach and screened parameters, are presented in Fig. 6. The properties of the excited states contributing to these spectra are displayed in table III. Before discussing the many-particle wave functions of various excited states, it is important to specify that for PDPA-5, orbitals $H-17/L+17$ and $H-19/L+19$ appearing in various states are the substituent phenyl-ring-based d/d^* orbitals making important contributions to the transverse THG spectra computed using the Hückel model (cf. sec. III A 2). It is obvious from Fig. 6 that: (a) For PDPA-5 four states labeled n_yB_u, k_yB_u, j_yA_g, and m_yA_g (subscript y implies y, i.e., transverse direction) contribute to the spectrum, while (b) for PPV-2 three states $1B_u$, jA_g, and mA_g make main contributions. Furthermore, the main contributions to the intensities of the THG spectra of both the substances are from two A_g-type peaks: j_yA_g and m_yA_g for PDPA-5, and jA_g and mA_g for PPV-2. For PDPA, we recall that at the Hückel model level, the transverse THG spectrum had only one peak due to closely-spaced A_g-type states corresponding to a single-particle excitation from the orbitals near the Fermi level (H/L) to the phenyl-based d/d^* orbitals. Upon examining the many-particle wave functions of various excited states of PDPA-5, we conclude that even at the many-body level the excited states contributing to the transverse THG spectra originate from the same set of single excitations involving H/L and phenyl-based d/d^* orbitals except for the $k_yB_u$state. However, the charge-density analysis of the orbitals involved in the k_yB_u state reveals that the orbitals in question ($H-3/L+3$, $H-4/L+4$) have significant charge density on the substituent phenyls. Thus, we can safely conclude that in the transverse THG spectrum of PDPA-5, the substituent-phenyl-based orbitals play a very important role. On comparing the many-particle wave functions of the A_g-type states contributing to the THG spectra of the two systems, we find that unlike the case of PDPA-5, in PPV-2 these states (kA_g and mA_g) have important contributions from the two-particle excitations

as well. However, the contributions of the single-particle excitations to these states in both PDPA-5 and PPV-2 have similar character—they involve H/L orbitals and high-lying orbitals localized predominantly in the phenyl rings. Upon further investigation of these high-lying orbitals involved in single excitations we conclude that they are of d/d^*-type phenyl-based orbitals. Therefore, we conclude that the mechanism of the transverse THG in PDPA's has noticeable similarities to that of THG in *trans*-stilbene.

Finally, in Fig. 7, we compare the transverse THG spectrum of PDPA-5 with its longitudinal one, both computed using the MRSDCI procedure, and the screened parameters. It is clear from the figure that the most intense peak in the transverse spectrum is about half in intensity as compared to the strongest peak in the longitudinal one, and is located in the higher energy range where there is no competing longitudinal response. Thus, our PDPA-5 calculations suggest that the transverse THG response of these materials, compared to their longitudinal response, is significant, as well as clearly distinguishable from it, in an experiment. However, it remains to be verified whether the results obtained for small oligomers will also be valid for the bulk PDPA's.

IV. CONCLUSIONS

Our aim behind undertaking the present theoretical study of the nonlinear optical properties of the novel polymer PDPA was, not only to calculate their THG spectra, but also to understand the underlying mechanism in a way similar to what has been possible for simpler polymers such as *trans*-polyacetylene,[2,3] PPP, and PPV.[9,24] This understanding has chiefly arisen from the essential state mechanism alluded to earlier in section I, which aims to explain the nonlinear optical properties of chain-like,[2,3] and more recently phenylene-based conjugated polymers,[9] in terms of a small number of excited states. For PDPA's, whose structure has ingredients in common with both the chain-like as well as the phenyl-based polymers, our calculations suggest that their nonlinear optical properties can also be understood along the same lines as the essential state mechanism. However, because of the anisotropic nonlinear optical response of PDPA's stemming from their structural anisotropy, the essential states contributing to various components of susceptibility are different. Our independent-electron as well as correlated calculations suggest that the THG spectrum of PDPA's is distributed over two natural energy scales: (a) low-energy region of the spectrum has significant intensity mainly for the longitudinal component, while (b) high-energy region of the spectrum has intensity mostly for the transverse component. The longitudinal THG spectrum bears striking qualitative resemblance to the THG spectrum of polyenes with similar essential states contributing to the intensities therein. The transverse THG spectrum on the other hand, has resemblance to the THG spectrum of *trans*-stilbene, with again, similar type of essential states contributing to their intensities. The essential states which contribute to the longitudinal spectra of these polymers are quite distinct from the states contributing to their transverse spectra. The states contributing to the longitudinal spectra can be described in terms of chain-based orbitals close to the Fermi level, however, to describe the transverse spectra, one needs to take into account the excitations involving phenyl-based orbitals away from the Fermi level. Therefore, it will be of considerable interest if the theoretical predictions presented here can be tested in experiments.

V. ACKNOWLEDGMENTS

We are grateful to Sumit Mazumdar (University of Arizona) for a critical reading of the manuscript, and for many suggestions for improvement. These calculations were performed on the Alpha workstations of Physics Department, and the Computer Center, IIT Bombay.

[1] See, e.g., P.N Prasad and D.J. Williams, *Introduction to Nonlinear Optical Effects in Molecules and Polymers* (Wiley, New York, 1991).
[2] S.N. Dixit, D. Guo, and S. Mazumdar, Phys. Rev. B **43**, 6781 (1991).
[3] S. Mazumdar and F. Guo, J. Chem. Phys. **100**, 1665 (1994).
[4] V.A. Shakin, S. Abe, and T. Kobayashi, Phys. Rev. B **53**, 10656 (1996).
[5] S. Tretiak, V. Chernyak, and S. Mukamel, Phys. Rev. Letts. **77**, 4656 (1996).
[6] D. Yaron, Phys. Rev. B **54**, 4609 (1996).
[7] Z. Shuai, J.L. Bre'das, A. Saxena, and A.R. Bishop, J. Chem. Phys. **109**, 2549 (1998).
[8] A. Chakrabarti and S. Mazumdar, Phys. Rev. B **59**, 4839 (1999).
[9] M. Y. Lavrentiev, W. Barford, S.J. Martin, H. Daly, and R.J. Bursill, Phys. Rev. B **59**, 9987 (1999).
[10] K. Tada, R. Hidayat, M. Hirohata, M. Teraguchi, T. Masuda and K. Yoshino, Jpn. J. Appl. Phys., part 2 **35**, L1138 (1996).
[11] K. Tada, R. Hidayat, M. Hirohata, H. Kajii, S. Tatsuhara, A. Fujii, M. Ozaki, M. Teraguchi, T. Masuda and K. Yoshino, Proc. SPIE-Int. Soc. Opt. Eng., **3145**, 171 (1997).
[12] M. Liess, I. Gontia, T. Masuda, K. Yoshino, and Z.V. Vardeny, Proc. SPIE-Int. Soc. Opt. Eng., **3145**, 179 (1997).
[13] A. Fujii, M. Shkunov, Z.V. Vardeny, K. Tada, K. Yoshino, M. Teraguchi and T. Masuda, Proc. SPIE-Int. Soc. Opt. Eng., **3145**, 533 (1997).
[14] I. Gontia, S.V. Frolov, M. Liess, E. Ehrenfreund, Z.V. Vardeny, K. Tada, H. Kajii, R. Hidayat, A. Fujii, K. Yoshino, M. Teraguchi and T.Masuda, Phys. Rev. Lett. **82**, 4058

A. Shukla: Fig 1

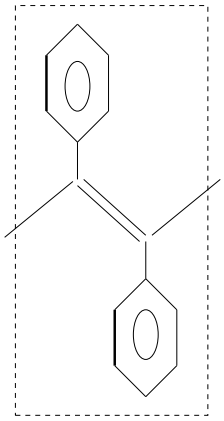


Figure 1: The unit cell of PDPA. The phenyl rings are rotated with respect to the y-axis, which is transverse to the axis of the polyene backbone (x-axis)

(1999).
[15] R. Sun, Y. Wang, X. Zou, M. Fahlam, Q. Zheng, T. Kobayashi, T. Masuda and A.J. Epstein, Proc. SPIE-Int. Soc. Opt. Eng., **3476**, 332 (1998).
[16] R. Hidayat, S. Tatsuhara, D.W. Kim, M. Ozaki, K. Yoshino, M. Teraguchi and T. Masuda, Phys. Rev. B **61**, 10167 (2000).
[17] A. Fujii, R. Hidayat, T. Sonoda, T. Fujisawa, M. Ozaki, Z.V. Vardeny, M. Teraguchi, T. Masuda, and K. Yoshino, Synth. Met. **116**, 95 (2001).
[18] A. Shukla and S. Mazumdar, Phys. Rev. Lett **83**, 3944 (1999).
[19] H. Ghosh, A. Shukla, and S. Mazumdar, Phys. Rev. B **62**, 12763 (2000).
[20] A. Shukla, H. Ghosh, and S. Mazumdar, Synth. Met. **116**, 87 (2001).
[21] K. Ohno, Theor. Chim. Acta **2**, 219 (1964).
[22] M. Chandross and S. Mazumdar, Phys. Rev. B **55**, 1497 (1997).
[23] A. Shukla, Phys. Rev. B **65**, 125204 (2002).
[24] A. Shukla, H. Ghosh, and S. Mazumdar, Phys. Rev. B **67**, 245203 (2003).
[25] J. Yu and W.P. Su, Phys. Rev. B **44**, 13315 (1991).
[26] B.J Orr and J.F. Ward, Mol. Phys. **20**, 513 (1971).
[27] The many-particle wave functions of half-filled conjugated polymers such as PDPA exhibit particle-hole (charge conjugation) symmetry when treated using the models such as the Hubbard model and the PPP model. Therefore, for every configuration which contributes to its wave function, its charge-conjugated (c.c.) counterpart will contribute in equal measure. For example, if configuration $|H \rightarrow L+1\rangle$ occurs in the wave function with coefficient 0.69, configuration $|H-1 \rightarrow L\rangle$ will also occur in the wave function with coefficient of the same magnitude (although, the sign could be reversed). Thus, we will use shorthand notation $|H \rightarrow L+1\rangle + c.c.$ (0.69) to denote the contribution of these configurations to the wave function. Above, H/L refer to HOMO/LUMO orbitals.

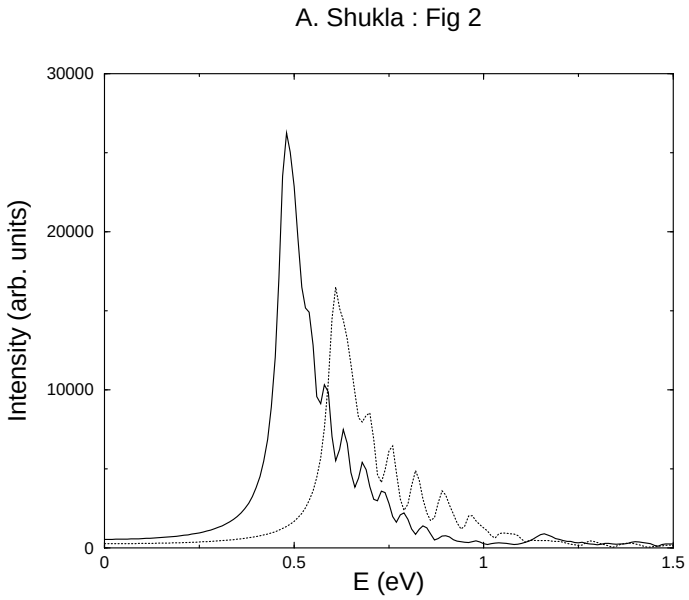


Figure 2: Comparison of $|\chi^{(3)}_{xxxx}(-3\omega;\omega,\omega,\omega)|$ of PDPA (solid line) and *trans*-polyacetylene (dotted line) oligomers containing fifty unit cells, computed using the Hückel model. Linewidth of 0.05 eV was assumed for all energy levels.

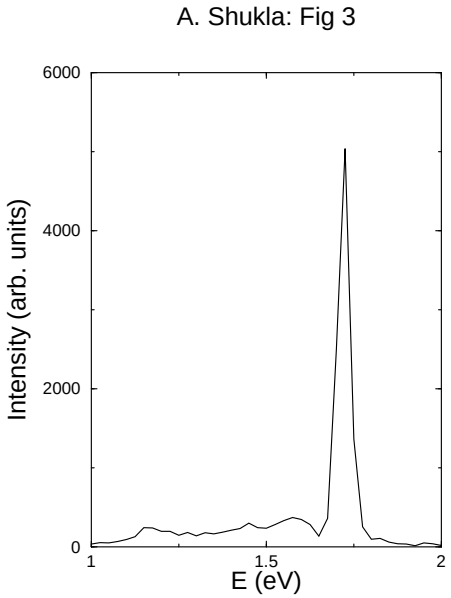


Figure 3: $|\chi^{(3)}_{yyyy}(-3\omega;\omega,\omega,\omega)|$ of PDPA-30 plotted as a function of incident photon energy. Linewidth of 0.05 eV was assumed for all energy levels.

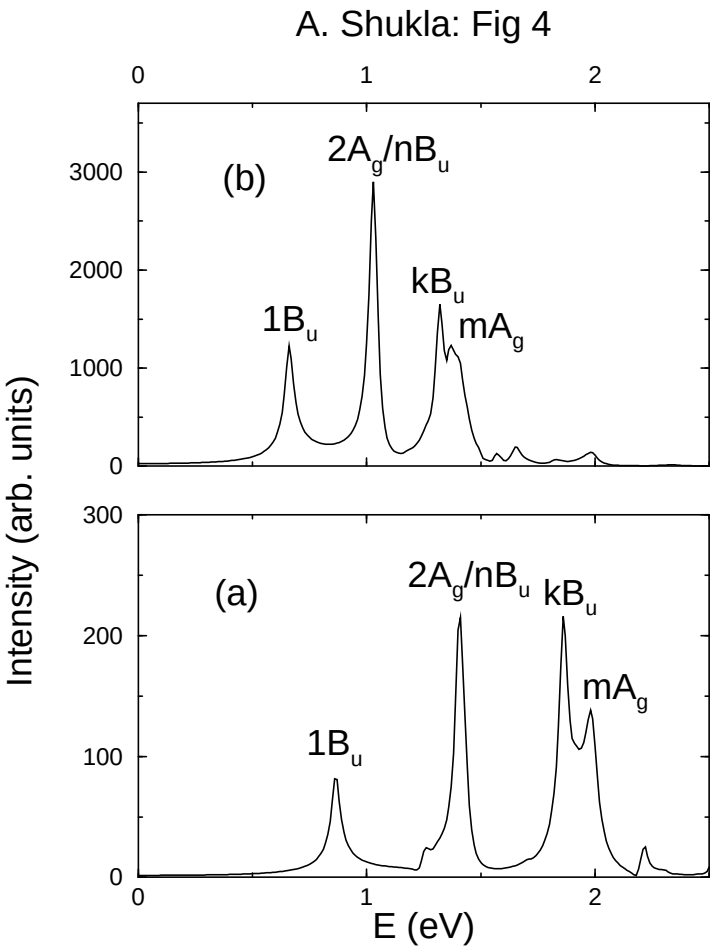


Figure 4: The magnitudes of the longitudinal component of the third-harmonic generation spectra ($|\chi^{(3)}_{xxxx}(-3\omega;\omega,\omega,\omega)|$) of oligo-PDPA's computed using the QCI approach and the screened parameters for: (a) PDPA-5 (b) PDPA-10. A linewidth of 0.05 eV was assumed for all the levels.

Table I: Excited states contributing to the longitudinal THG spectrum of PDPA-5 and PDPA-10 as obtained in QCI calculations. Under the heading wave function, we list the most important configurations contributing to the many-body wave function of the state concerned, along with their coefficients, consistent with our convention[27].

	PDPA-5		PDPA-10	
State	Energy (eV)	Wave Function	Energy (eV)	Wave Function
$2A_g$	2.86	$\|H\rightarrow L+1\rangle + c.c.$ (0.57) $\|H\rightarrow L; H\rightarrow L\rangle$(0.48)	2.08	$\|H\rightarrow L+1\rangle + c.c.$ (0.49) $\|H\rightarrow L; H\rightarrow L\rangle$(0.50)
mA_g	3.98	$\|H\rightarrow L+1\rangle + c.c.$(0.37) $\|H\rightarrow L; H\rightarrow L\rangle$(0.74)	2.82 ($3A_g$) 2.88 ($4A_g$)	$\|H\rightarrow L+1\rangle + c.c.$(0.68) $\|H\rightarrow L; H\rightarrow L\rangle$(0.37)
$1B_u$	2.59	$\|H\rightarrow L\rangle$(0.99)	1.98	$\|H\rightarrow L\rangle$(0.96)
nB_u	4.21	$\|H-1\rightarrow L+1\rangle$(0.94) $\|H\rightarrow L; H\rightarrow L+1\rangle + c.c.$(0.14)	3.08	$\|H-1\rightarrow L+1\rangle$(0.72) $\|H\rightarrow L+2\rangle + c.c.$(0.38)
kB_u	5.58	$\|H\rightarrow L; H\rightarrow L+1\rangle + c.c.$(0.57) $\|H-1\rightarrow L+1; H-1\rightarrow L\rangle + c.c.$(0.25) $\|H-1\rightarrow L+1\rangle$(0.19)	3.96	$\|H-2\rightarrow L+2\rangle$(0.59) $\|H\rightarrow L; H\rightarrow L+1\rangle + c.c.$(0.31) $\|H-1\rightarrow L+1; H-1\rightarrow L\rangle + c.c.$(0.23)

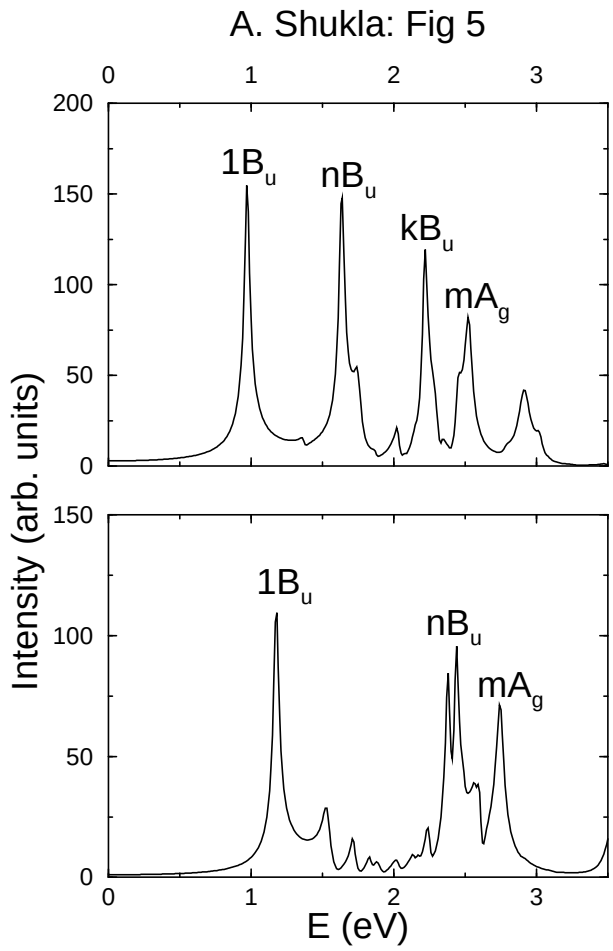


Figure 5: The magnitude of the third-harmonic generation spectrum ($|\chi^{(3)}_{xxxx}(-3\omega;\omega,\omega,\omega)|$) of: (a) PDPA-10 (top) and (b) ten unit oligomer of *trans*-polyacetylene (bottom) computed using the QCI approach and the standard parameters. A linewidth of 0.05 eV was assumed for all the levels.

Table II: Comparison of excited states of ten unit polyene (PA-10) and PDPA-10 computed using the QCI method and the standard parameters in the P-P-P Hamiltonian. Rest of the information is the same as given in the caption of table I.

	PDPA-10		PA-10	
State	Energy (eV)	Wave Function	Energy (eV)	Wave Function
$1B_u$	2.91	$\|H \rightarrow L\rangle(0.90)$ $\|H-1 \rightarrow L+1\rangle(0.32)$	3.53	$\|H \rightarrow L\rangle(0.82)$ $\|H-1 \rightarrow L+1\rangle(0.28)$
mA_g	5.05	$\|H \rightarrow L; H \rightarrow L\rangle(0.47)$ $\|H \rightarrow L; H-1 \rightarrow L+1\rangle(0.45)$ $\|H \rightarrow L+1\rangle + c.c.(0.33)$	5.49	$\|H \rightarrow L+1\rangle + c.c.(0.42)$ $\|H \rightarrow L; H \rightarrow L\rangle(0.36)$ $\|H \rightarrow L; H-1 \rightarrow L+1\rangle(0.31)$
nB_u	4.90	$\|H-1 \rightarrow L+1\rangle(0.62)$ $\|H \rightarrow L+2\rangle + c.c.(0.29)$	7.31	$\|H \rightarrow L; H \rightarrow L+1\rangle + c.c.(0.28)$ $\|H \rightarrow L; H-1 \rightarrow L+2\rangle + c.c.(0.27)$ $\|H-1 \rightarrow L+1\rangle(0.23)$
kB_u	6.65	$\|H \rightarrow L; H \rightarrow L+1\rangle + c.c.(0.36)$ $\|H-1 \rightarrow L+1\rangle(0.29)$ $\|H-2 \rightarrow L+2\rangle(0.20)$		

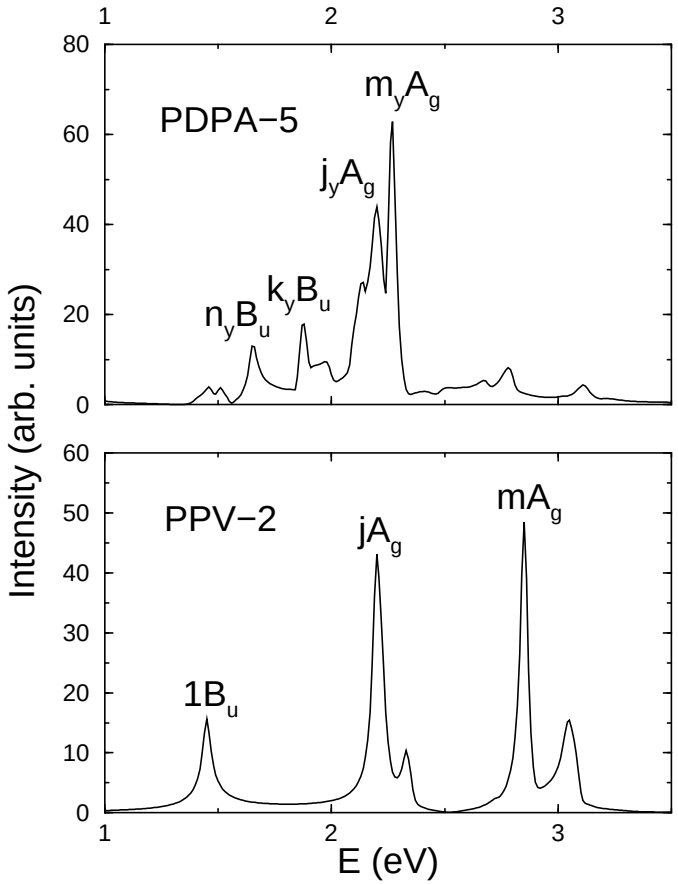


Figure 6: Comparison of transverse third-harmonic generation spectra of PDPA-5 with that of *trans*-stilbene (PPV-2) oriented along the y-axis. Both the spectra were computed using the screened parameters. For PDPA-5, MRSDCI method was used, while for PPV-2, QCI method was used. A linewidth of 0.05 eV was assumed for all the levels.

Table III: Nature of excited states contributing to the transverse THG spectrum of PDPA-5 computed by MRSDCI method. Rest of the information is same as given in the caption of table I.

PDPA-5			PPV-2		
State	Energy (eV)	Wave Function	State	Energy (eV)	Wave Function
j_yA_g	4.39	$\|H \rightarrow L+17\rangle + c.c$ (0.43) $\|H \rightarrow L+19\rangle + c.c$ (0.43)	jA_g	4.45	$\|H \rightarrow L+3\rangle + c.c$ (0.43) $\|H \rightarrow L; H \rightarrow L\rangle + c.c$ (0.42)
m_yA_g	4.52	$\|H \rightarrow L+17\rangle + c.c$ (0.27) $\|H \rightarrow L+19\rangle + c.c$ (0.38) $\|H-2 \rightarrow L+1\rangle + c.c$ (0.30)	mA_g	5.72	$\|H-1 \rightarrow L+1; H \rightarrow L\rangle$(0.29) $\|H-2 \rightarrow L+2; H \rightarrow L\rangle$(0.29) $\|H \rightarrow L+3\rangle + c.c.$(0.26) $\|H \rightarrow L+5\rangle + c.c.$(0.25)
n_yB_u	4.96	$\|H \rightarrow L+19\rangle + c.c.$(0.60)	$1B_u$	4.35	$\|H \rightarrow L\rangle$(0.90)
k_yB_u	5.61	$\|H-3 \rightarrow L+3\rangle$(0.56) $\|H-4 \rightarrow L+4\rangle$(0.49)			

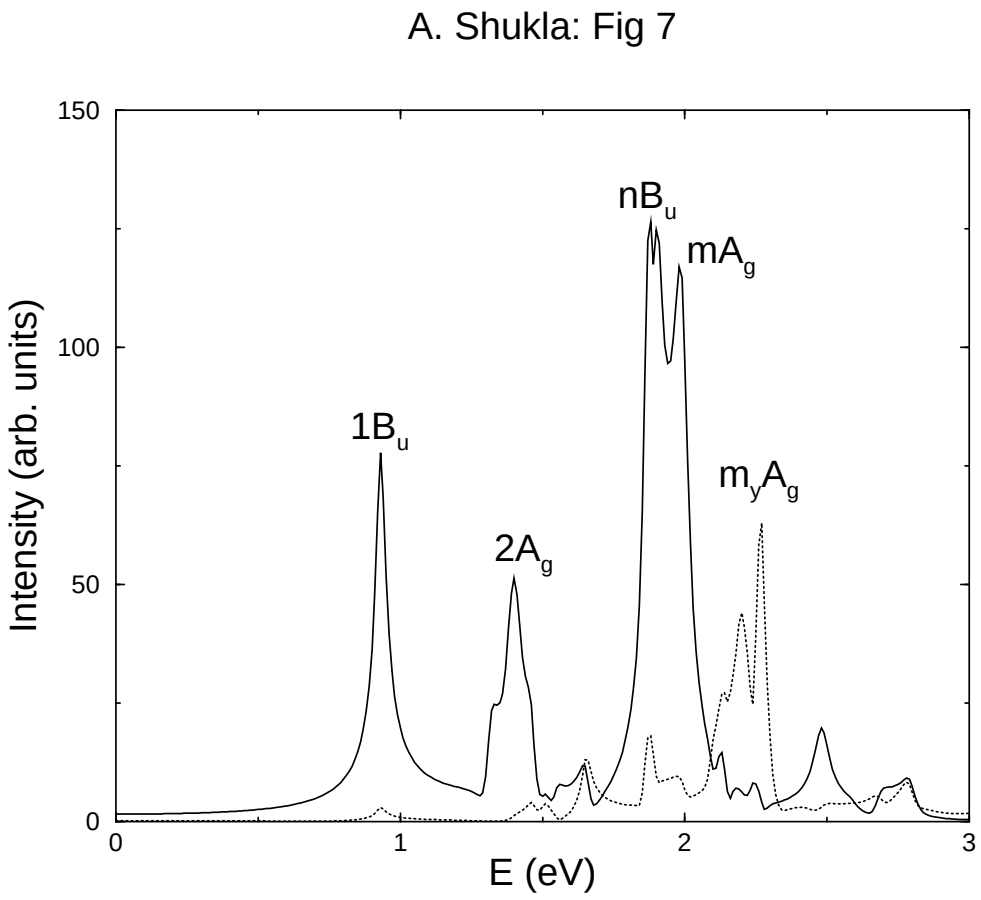


Figure 7: Comparison of longitudinal (solid lines) and the transverse (dotted lines) third-harmonic generation spectra of PDPA-5 computed using the screened parameters and the MRSDCI method. A linewidth of 0.05 eV was assumed for all the levels.